Bioorganic & Medicinal Chemistry 18 (2010) 5925–5931

Contents lists available at ScienceDirect

Bioorganic & Medicinal Chemistry

journal homepage: www.elsevier.com/locate/bmc

Comparison of MRI properties between derivatized DTPA and DOTA gadolinium–dendrimer conjugates

K. Nwe [a], M. Bernardo [c], C. A. S. Regino [b], M. Williams [b], M. W. Brechbiel [a,*]

[a] Radioimmune & Inorganic Chemistry Section, Radiation Oncology Branch, National Cancer Institute, 10 Center Drive, Bethesda, MD 20892, United States
[b] Molecular Imaging Program, National Cancer Institute, 10 Center Drive, Bethesda, MD 20892, United States
[c] Research Technology Program, SAIC-Frederick, Inc., NCI-Frederick, Frederick, MD 21702, United States

ARTICLE INFO

Article history:
Received 26 April 2010
Revised 23 June 2010
Accepted 25 June 2010
Available online 8 July 2010

Keywords:
2-(*p*-Isothiocyanato benzyl)-6-methyl-diethylenetriaminepentaacetic acid (1B4M-DTPA)
Polyamidoamine (PAMAM) generation 4 dendrimer (G4D)
2-(4-Isothiocyanatobenzyl)-1,4,7,10-tetraazacyclododecane-*N*,*N*′,*N*″,*N*‴-tetraacetic acid gadolinium complex (*p*-SCN-*C*-DOTA[Gd])

ABSTRACT

In this report we directly compare the in vivo and in vitro MRI properties of gadolinium–dendrimer conjugates of derivatized acyclic diethylenetriamine-*N*,*N*′,*N*′,*N*″,*N*″-pentaacetic acid (1B4M-DTPA) and macrocyclic 1,4,7,10-tetraazacyclododecane-*N*,*N*′,*N*″,*N*‴-tetraacetic acid (*C*-DOTA). The metal–ligand chelates were pre-formed in alcohol prior to conjugation to the generation 4 PAMAM dendrimer (G4D), and the dendrimer-based agents were purified by Sephadex® G-25 column. The analysis and SE-HPLC data indicated chelate to dendrimer ratios of 30:1 and 28:1, respectively. Molar relaxivity measured at pH 7.4, 22 °C, and 3T are comparable (29.5 vs 26.9 mM^{-1} s^{-1}), and both conjugates are equally viable as MRI contrast agents based on the images obtained. The macrocyclic agent however exhibits a faster rate of clearance in vivo ($t_{1/2}$ = 16 vs 29 min). Our conclusion is that the macrocyclic-based agent is the more suitable agent for in vivo use for these reasons combined with kinetic inertness associated with the Gd(III) DOTA complex stability properties.

Published by Elsevier Ltd.

1. Introduction

Magnetic resonance imaging (MRI) has become a powerful diagnostic imaging modality owing to its non-invasive nature and superb spatial resolution at the sub-millimeter range.[1] During the development of this imaging modality, contrast agents have been employed to induce additional contrast and increase the sensitivity of the MRI scan.[1] The increased usage of MRI combined with the necessity for a contrast agent prompts the development of new efficient agents. Clinically used low molecular weight extracellular contrast agents such as $[Gd(DTPA)(H_2O)]^{-2}$ (Magnevist®) suffer from rapid extravasation from the blood vessels into interstitial spaces and fast decrease in concentration in the blood vessels combined with rapid whole body clearance.

The use of Gd(III) chelates conjugated to high molecular weight carriers such as a PAMAM dendrimer prolongs intravascular retention and circulation time, slows down molecular rotation which results in a short relaxation time, and increases in relaxivity.[2] Polyamidoamine (PAMAM) dendrimers of different generations conjugated to an acyclic diethylenetriaminepentaacetic acid (DTPA) derivative, 2-(*p*-isothiocyanato benzyl)-6-methyl-diethylenetriaminepentaacetic acid (1B4M-DTPA), are versatile in MRI applications due to their mono-dispersed nature and available range of molecular sizes.[3,4] Additionally, a good contrast agent must be non-cytotoxic, must have high water solubility most preferably at physiological pH, and high relaxivity properties.

In recent years, dendrimers have become a common platform for building multifunctional macromolecular nanomaterials to be used as diagnostic and therapeutic agents.[5] There have been reports indicating that dendrimers are applicable as carriers for site-specific delivery of drugs and that they do not alter the function of the molecules attached.[6–9] It has also been discovered that dendrimers can act as drugs themselves.[10–12] As an example, Supattapone et al. reported that branched polyamine dendrimers stimulate the removal of prion proteins present in infected cells. In the MRI field, dendrimers have not only allowed the molecules to retain their functions, but have also greatly enhanced the signal to noise ratio of the images; however, this has never reached its full potential.

The recent spate of reports regarding nephrogenic systemic fibrosis (NSF) linked to the use of Gd(III) DTPA derived MR contrast agents has provided our lab with an impetus for re-examination of the use of bifunctional DTPA agents for the creation of macromolecular MR agents not only in regards to simple stability

* Corresponding author. Address: Radioimmune & Inorganic Chemistry Section, Radiation Oncology Branch, NCI, NIH, Building 10, Room B3B69, 10 Center Drive, Bethesda, MD 20892-1088, United States. Tel.: +1 301 496 0591; fax: +1 301 402 1923.
E-mail address: martinwb@mail.nih.gov (M.W. Brechbiel).

0968-0896/$ - see front matter Published by Elsevier Ltd.
doi:10.1016/j.bmc.2010.06.086

aspects,[13–17] but also to the extended in vivo residence time associated with such agents as well as establishing comparable relaxivity properties. Clearly, stability requirements for macromolecular MR agents are great. Gd(DOTA) is known as a better contrast agent in terms of chemical stability and thus potentially less toxicity as compared to the currently used Gd(DTPA).[18,19] Gd(DOTA), DOTAREM™ has been extensively evaluated in patients with pre-existing renal diseases and to date has displayed no clinical side effects.[20] The higher relaxivity and stability of Gd(DOTA) makes it applicable as an alternative to Gd(DTPA) for MRI.[21] The formation and stability of the Gd(DOTA) complex has also been thoroughly studied and data indicate that the dissociation of the metal ion was exceedingly slow even at low pH (2–4), on the order of days,[22] while its thermodynamic stability was comparable to that of Gd(DTPA).[23] A previous study showed that Gd(DOTA) has five orders of magnitude higher in vitro stability as compared to Gd(DTPA), which can translate to lower in vivo toxicity.[18] No significance differences in enhancement of the brain image of rats were observed between Gd(DTPA) and Gd(DOTA), which also validates Gd(DOTA) as a potential CA for brain imaging.[24]

Herein we report the preparation and evaluation of two generation 4 dendrimer (G4D) based contrast agents, G4-(*C*-DOTA-Gd)$_{28}$ and G4-(1B4M-DTPA-Gd)$_{30}$ that meet criteria such as water solubility and high relaxivity. We also present here the applicability of the *C*-DOTA derivative (or an equivalent DOTA derivative) applied to complex Gd(III) as an agent of choice to replace usage of bifunctional DTPA agents employed to sequester Gd(III) as a component of macromolecular MR contrast agents.

In this report, the ligands are first used to sequester Gd(III) and thereafter the resulting metal complexes are covalently attached to the terminal –NH_2 groups of the G4D. We have recently reported that this method is significantly advantageous over conventional methods, wherein the metal ion is introduced and sequestered in the final step under aqueous conditions. The resulting product is more directly characterizable, and possesses an ~twofold enhancement of molar relaxivity when using a bifunctional DTPA chelating agent compared to a similar agent prepared by convention means while also being able to decrease the overall Gd(III) content by ~30%.[25] The PAMAM generation 4 dendrimer (G4D) with amine surface groups (–NH_2) was employed to build the dendrimer–metal chelate conjugates; G4D Gd(III) chelate conjugates are known to have moderate blood circulation time and relatively fast excretion via the kidney.[26] Hence, we hypothesized that the replacement of that bifunctional DTPA chelating agent with a suitable bifunctional DOTA chelating agent would not only address safety and toxicity issues, but perhaps also further enhance the molar relaxivity properties of our dendrimer-based MRI contrast agents. In addition to characterization and assessment of relaxivity properties of these agents, mice were imaged in pairs ($n = 2$) with both G4-(1B4M-DTPA-Gd)$_{30}$ and G4-(*C*-DOTA-Gd)$_{28}$ to directly compare the effect of the agents on the quality of MR imaging. To the best of our knowledge, this is one of the few studies to directly make such comparative studies.

2. Experimental

2.1. Materials and methods

Ethylenediamine core PAMAM dendrimer generation 4 (G4 dendrimer) in MeOH (10% w/v) was obtained from Dendritech. Gadolinium nitrate pentahydrate ($Gd(NO)_3{\cdot}5H_2O$) was purchased from Aldrich (St. Louis, MO). G4-(1B4M-DTPA-Gd)$_{30}$ was prepared and purified as previously reported.[25] 2-(4-nitrobenzyl)-1,4,7,10-tetraazacyclododecane-*N*,*N*′,*N*″,*N*‴-tetraacetic acid was prepared as the HCl salt.[27] Phosphate buffered saline (1× PBS) at pH 7.4 was obtained from Digene (Gaithersburg, MD). Size-exclusion HPLC (SE-HPLC) was performed using a Beckman System Gold® (Fullerton, CA) equipped with model 126 solvent delivery module and a model 166NMP UV detector (λ 254 nm) controlled by 32 Karat software. Size-exclusion chromatography was performed on a TSK-gel G3000PW 10 μm, 7.8 mm × 300 mm (Tosoh Bioscience, Montgomeryville, PA), with a TSK-gel 10 μm guard column (Tosoh Bioscience, Montgomeryville, PA) using phosphate buffered saline (1× PBS) solution as the eluent at 0.5 mL/min, respectively. Reverse-phase HPLC (RP-HPLC) was performed by using a Beckman System Gold HPLC equipped with 168 UV–vis detector with peak detection at 254 and 280 nm and a C_{18} Varian microsorb™-mv column (250 × 4.6 mm; 5 μm). A gradient system composed of a pH 9.0 buffer (50 mM triethylamine/acetic acid) and methanol (25 min linear gradient from 0% to 100% methanol) with a flow rate of 1 mL/min was employed. All water used was purified using a Hydro Ultrapure Water Purification system (Rockville, MD). The Sephadex® G-25 resin was purchased from Pharmacia (Sweden), pre-treated with 1× PBS, and loaded to a Pharmacia Biotech column 2.6 × 39.7 cm (Uppsala, Sweden). Elemental analyses were performed by Galbraith Laboratories, Inc. (Knoxville, TN) using combustion analysis method for *C, H, N*, inductively coupled plasma-optical emission spectroscopy (ICP-OES) method for determining the *S*, and inductively coupled plasma-mass spectrometry (ICP-MS) for *Gd*. The Bio-Rad gel filtration standard used to compare the molecular weight of the dendrimer conjugate was purchased from Bio-Rad (Hercules, CA).

2.2. Syntheses

2.2.1. 2-(4-Nitrobenzyl)-1,4,7,10-tetraazacyclododecane-*N*,*N*′,*N*″,*N*‴-tetraacetic acid gadolinium complex (*p*-NO_2-*C*-DOTA[Gd]) (1)

0.44 g (0.68 mmol) of *C*-DOTA·3HCl ligand and 0.31 g (0.71 mmol) of $Gd(NO_3)_3{\cdot}5H_2O$ in MeOH (20 mL) were refluxed for 8 h. The solvent was reduced to 1.5 mL and CH_2Cl_2 was added until an oil suspension formed. The oil was separated and dried under vacuum to yield a pale yellow solid (0.54 g; 85%). ESI *m*/*e*: calcd for $C_{23}H_{33}N_5O_{10}Gd$; 697. Found 693 (M^{-1}). RP-HPLC t_R = 12.6 min. % Calcd for $C_{23}H_{33}N_5O_{10}Gd{\cdot}2NO_3{\cdot}3HCl$: C, 29.69; H, 3.87; N, 10.54. Found: C, 29.64; H, 3.89; N, 10.49.

2.2.2. 2-(4-Aminobenzyl)-1,4,7,10-tetraazacyclododecane-*N*,*N*′,*N*″,*N*‴-tetraacetic acid gadolinium complex (*p*-NH_2-*C*-DOTA[Gd]) (2)

A solution of compound **1** (2.01 g; 2.16 mmol) and 10% Pd/C (0.4 g) in H_2O (40 mL) was placed in a Parr hydrogenator at 15 psi for 4 h. (The completion of the reaction was confirmed by RP-HPLC.) The mixture was filtered on a glass frit through a pad of Celite (Celite® 535 Coarse; Fluka) and washed with H_2O (20 mL). The filtrate was evaporated under high vacuum to afford compound **2** (1.73 g; 87%) as a yellow solid. ESI *m*/*e*: calcd for $C_{23}H_{35}N_5O_8Gd$; 667. Found 663 (M^{-1}). % Calcd for $C_{23}H_{35}N_5O_8Gd{\cdot}2NO_3{\cdot}3HCl{\cdot}H_2O$: C, 23.45; H, 3.99; N, 9.52. Found: C, 23.30; H, 4.20; N, 9.45. RP-HPLC t_R = 10.2 min.

2.2.3. 2-(4-Isothiocyanatobenzyl)-1,4,7,10-tetraazacyclododecane-*N*,*N*′,*N*″,*N*‴-tetraacetic acid gadolinium complex (*p*-SCN-*C*-DOTA[Gd]) (3)

A solution of 1 mL of thiophosgene in CH_2Cl_2 (10 mL) was added drop wise into a solution of compound **2** (2.00 g, 2.18 mmol) in H_2O (15 mL) at room temperature. The mixture was stirred for 1 h after the addition was complete. The organic phase was separated and the aqueous phase was washed with CH_2Cl_2 (10 mL) to remove the residue of thiophosgene. The aqueous was dried under vacuo to afford compound **3** as a yellow solid (0.93 g; 88%). ESI *m*/*e*: calcd for $C_{24}H_{33}N_5SO_8Gd$; 709. Found 705 (M^{-1}). % Calcd for

$C_{24}H_{33}N_5$ $SO_8Gd{\cdot}2NO_3{\cdot}3HCl{\cdot}H_2O$: C, 29.94; H, 3.80; N, 10.44. Found: C, 29.82; H, 3.81; N, 10.53. RP-HPLC t_R = 18.4 min.

2.2.4. Conjugation of G4 with 3—(G4-(*C*-DOTA-Gd)$_{28}$)

G4 PAMAM dendrimer (1.34 g, 0.0145 mmol; 15.35% w/w) in a 500 mL round bottom flask was dried under vacuum to remove the MeOH. The flask was charged with 350 mL of 1× conjugation buffer with EDTA (0.96 M $NaHCO_3$; 0.04 M Na_2CO_3; 3.0 M NaCl: 0.01 M EDTA) (pH ~8.5). Compound **3** (1.51 g, 1.57 mmol) was added in portions while the pH was adjusted to 8.5 with 1 M NaOH. The mixture was stirred at room temperature for 5 d and 35 °C for 1 d. The solution was cooled to room temperature and filtered through a 0.45 μm cellulose acetate membrane filter (Corning, NY). The solvent was reduced under high vacuum to ~30 mL at room temperature. The dendrimer–chelate was purified by a Sephadex® G-25 column eluted with water (pH 7.5; the pH was adjusted to 7.5 with 1 M NaOH). The first band was collected and lyophilized to yield the conjugate as a yellowish fluffy solid (0.35 g; 65% based on dendrimer). SE-HPLC t_R = 14.7 min. % Calcd for $C_{622}H_{1250}N_{250}O_{125}{\cdot}28(C_{23}H_{30}N_4SO_{10}Gd){\cdot}51(Na){\cdot}55(H_2O)$: 42.89 (C), 6.31 (H), 15.08 (N), 2.47 (S), 12.16(Gd). Found: 42.93, 6.19, 15.19, 2.52, 11.96.

2.3. Molar relaxivity measurements

Stock solutions of the G4 dendrimer agents, G4(1B4M-DTPA-Gd)$_{30}$ and G4(*C*-DOTA-Gd)$_{28}$ (5.0 mM in Gd), were diluted to concentrations of 0.1, 0.25, 0.50, 0.75, and 1.0 mM in 1× PBS (300 μL). Solutions of Gd(III)-DTPA (Magnevist™; Bayer, Montville, NJ) at 0.25, 0.50, 0.75, 1.0, and 2.0 mM were prepared in 1× PBS (300 μL) and used as a reference standard. Relaxivity measurements were obtained at ~22 °C using a 3-Tesla clinical scanner (Signa Excite, GE Medical System, Waukesha, WI) equipped with a rectangular single loop receiver coil (84 × 126 × 6 mm). A series of single slice 2D inversion recovery (IR) fast spin echo images of all the solutions were acquired at the same time with a TE around 9 ms and using different inversion recovery times (TI = 50, 100, 350, 750, 1250, 2500, and 5000 ms) followed by a single slice 8-echo SE image (TE = 9 ms). The R_1 values for each dilution were determined by fitting ROI intensity values from variable IR images using Igor Pro (http://www.wavemetrics.com). R_2 values were measured from ROI values from T_2 maps, which were calculated from the multi-echo images in ImageJ (http://rsb.info.nih.gov/ij) using the MRI analysis plug-in (http://rsb.info.nih.gov/ij/plugins/mri-analysis.html). The molar relaxivities, r_1 and r_2, were obtained from the slope of $1/T_1$ or $1/T_2$ versus [Gd(III)] plots determined from region of interest measurements.

2.4. In vivo magnetic resonance imaging (MRI)

All animal studies were performed in accordance with the NIH guidelines for the humane use of animals and all procedures were reviewed and approved by the National Cancer Institute Animal Care and Use Committee. Normal 6–8 week old female nude mice (Charles Rivers Laboratories) were imaged two at a time to increase throughput using a 3T clinical scanner (Achieva, Philips Healthcare, Best, Holland) equipped with a dual mouse coil comprised of two parallel receive-only coils (saddle-shaped Helmholtz coils, 38 mm in diameter × 70 mm in length) connected to independent receiver channels and spaced 43 mm apart. Each mouse was placed in a physical restraint while a catheter line (30 gauge needle on a 0.010″ ID × 6″ long Tygon tubing) filled with 1× PBS was inserted into the tail vein, anesthetized using gas mixtures of 3% isoflurane in O_2, and then carefully placed in a mouse bed equipped with a nose cone, respiratory pad, and fiber optic temperature sensor for physiology monitoring. The mice were positioned in the dual mouse coil which was heated with air to maintain the mice at 34 °C. The anesthesia gas was adjusted between 1.5–2.5% isoflurane to maintain a respiration rate of ~30 bpm during the acquisition of all images. After acquiring a tri-planar gradient echo survey, a coronal view T_1-weighted 3D-fast spoiled gradient echo image with a low flip angle (repetition time of 14 ms, echo time of 2.4 ms, flip angle of 5°, field of view of 80 mm, matrix size of 512 × 512 pixels, 40 slices, slice thickness of 0.6 mm and 1 average; scan time of 2.3 min) was acquired followed by a dynamic series using a higher flip angle of 24° repeated every 2.5 min for one hour. The contrast agent was injected (50 μL of 6 mM stock solution in 1× PBS based on Gd(III) pushed with 50 μL of 1× PBS) after the first dynamic image at a rate of 150 μL/min using a syringe pump (BS-9000-8, Braintree Scientific, Braintree, MA). Blood clearance rates were determined from ROI intensity measurements of the jugular vein in the low flip angle image and high flip angle dynamic images using Image J. The intensity values during the dynamic scans were then converted to Gd(III) concentration and the resulting [Gd] time curves were fitted to a single exponential function using an Igor Pro (Wavemetrics) macro.

3. Results

Preparation of the G4-(1B4M-DTPA-Gd)$_{30}$ has been reported elsewhere.[25]

The preparative scheme leading to the formation of the conjugate G4-(*C*-DOTA-Gd)$_{28}$ is shown in Figure 1. The Gd(III) complex **1** was prepared by treatment of the ligand *C*-DOTA with $Gd(NO_3)_3{\cdot}5H_2O$ in methanol. Complex **1** could also be prepared by incubation of the ligand with $Gd(NO_3)_3{\cdot}5H_2O$ in H_2O with the pH maintained at 5.5, but preparation of the Gd(III) complex in methanol was chosen as a more convenient route, especially for ligands that have limited solubility in water. Our previous study showed that the Gd(III)-1B4M-DTPA complex formed in methanol gave a more stable complex than the one formed under aqueous condition.[25] Therefore, to maintain comparability between the two macromolecular agents, this aspect was held constant.

The reduction of the nitro group to amine was rapidly accomplished (Parr hydrogenator at 15 psi within ~4 h). Under these conditions neither cleavage of the nitrobenzyl group (over-reduction product) nor any dissociation of the metal ion from the ligand cavity were observed. A mixture of thiophosgene in CH_2Cl_2 was added drop wise to form complex **3** and the reaction was allowed to stir for 1 h thereafter, which was sufficient to complete this reaction. This brief reaction time also serves to eliminate extended exposure of the metal complex to low pH (1–2) conditions, which might induce dissociation of Gd(III) from the complex. After conjugation, the dendrimer-based conjugate was purified by a Sephadex® G-25 column. As noted in our previous report, this method proved to be more efficient as compared to the exhaustive and time consuming transverse-flow filtration (TFF) method.[25,26]

A plot of the inverse of longitudinal relaxation time ($1/T_1$) versus Gd(III) concentration for the G4(*C*-DOTA-Gd)$_{28}$ conjugate (0.1–1 mM), G4(1B4M-DTPA-Gd)$_{30}$ conjugate (0.1–1 mM) and Magnevist™ (0.25–2 mM) is shown in Figure 2. The data showed that the relaxivity of the two dendrimer-based agents is 6–7 times higher than that of Magnevist™. The in vivo average blood clearance rates were measured at the jugular vein for the two agents with the clearance data fit to a single exponential decay (Fig. 3). Table 1 summarizes the overall results for the two agents. G4-(1B4M-DTPA-Gd)$_{30}$ and G4-(*C*-DOTA-Gd)$_{28}$ have comparable values of dendrimer to chelate ratio (1:30 vs 1:28) as well as for molar relaxivity (29.5 vs 26.9), while the gap between the blood clearance half-lives is rather large (16.2 vs 29.1 min).

Dynamic contrast-enhanced MR images of the two agents at 16–23 min post-injection are shown in Figure 4. While one notes

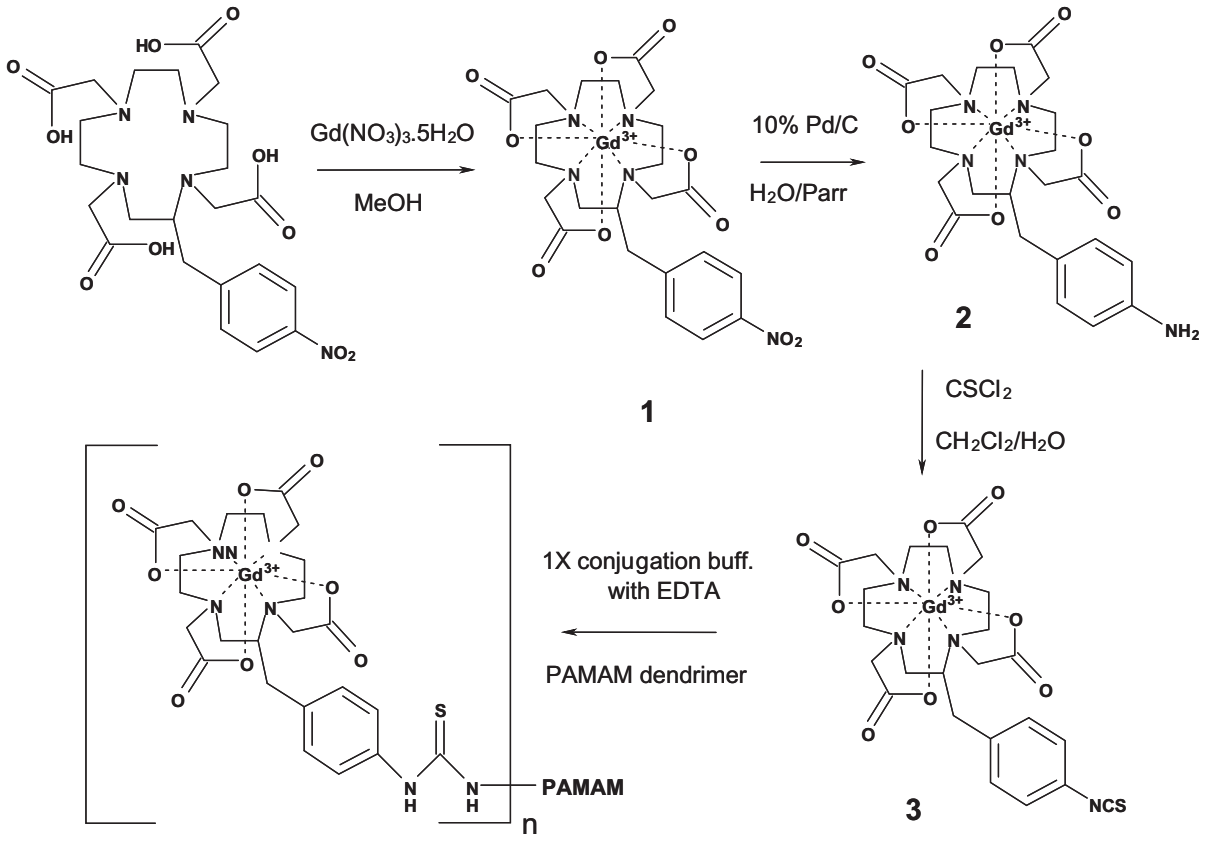

Figure 1. Synthetic scheme for G4-(*C*-DOTA-Gd)$_{28}$ conjugate.

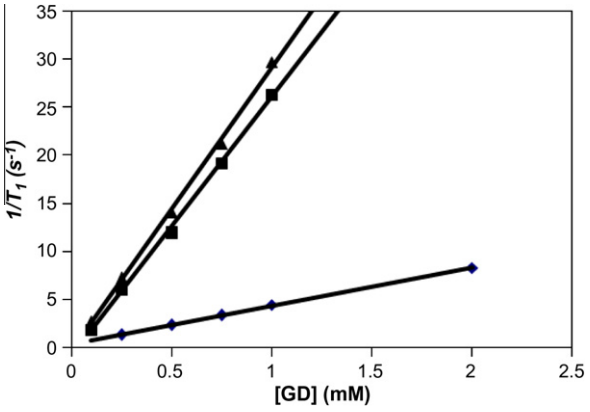

Figure 2. Molar relaxivity plots of G4-(*C*-DOTA-Gd)$_{28}$ (▲; 29.5 mM^{-1} s^{-1}), G4-(1B4M-DTPA-Gd)$_{30}$ (■; 26.9 mM^{-1} s^{-1}), and Magnevist (♦; 4.2 mM^{-1} s^{-1}).

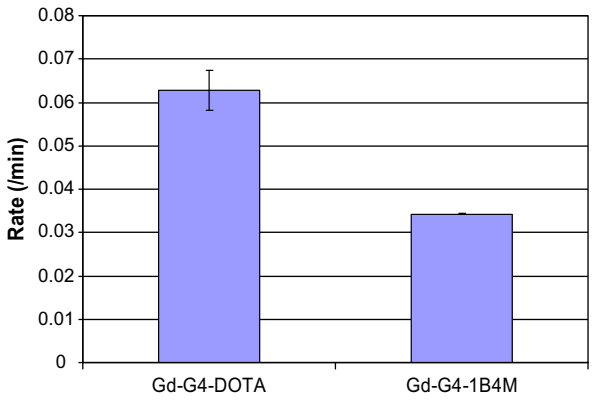

Figure 3. Average blood clearance rates measured at the jugular vein of G4-(1B4M-DTPA-Gd)$_{30}$ and G4-(*C*-DOTA-Gd)$_{28}$.

that the image quality of the two agents obtained in normal mice is similar, their circulation properties are different. Figure 5 shows the images of kidney obtained before and after injection of agents. Obviously the post-contrast images are different from the pre-contrast one as expected as well the images obtained for the two agents.

4. Discussion

As previously noted, formation of thermodynamically stable lanthanide complexes with DOTA is slow,[22,28,29] but the complexes formed are extremely stable.[30] A stability constant of 10^{28} was reported for Gd(DOTA)$^{-1}$ as opposed to 10^{22} for Gd(DTPA)$^{-1}$.[31] Comparison of MRI properties between derivatized DTPA and DOTA gadolinium–dendrimer conjugates, lanthanide complex formation and dissociation kinetics with DOTA ligand are usually studied under aqueous condition as cited above. However, in our study the complexes are formed in methanol. Therefore, at this point whether the mechanism and number of steps involved in complex formation as well as whether dissociation is the same as proposed for aqueous condition is under study.

The surface amine groups of polyamidoamine (PAMAM) dendrimers are known to be positively charged at physiological pH. Previous reports demonstrated faster clearance of non-specific binding PAMAM dendrimers due to electrostatic interaction

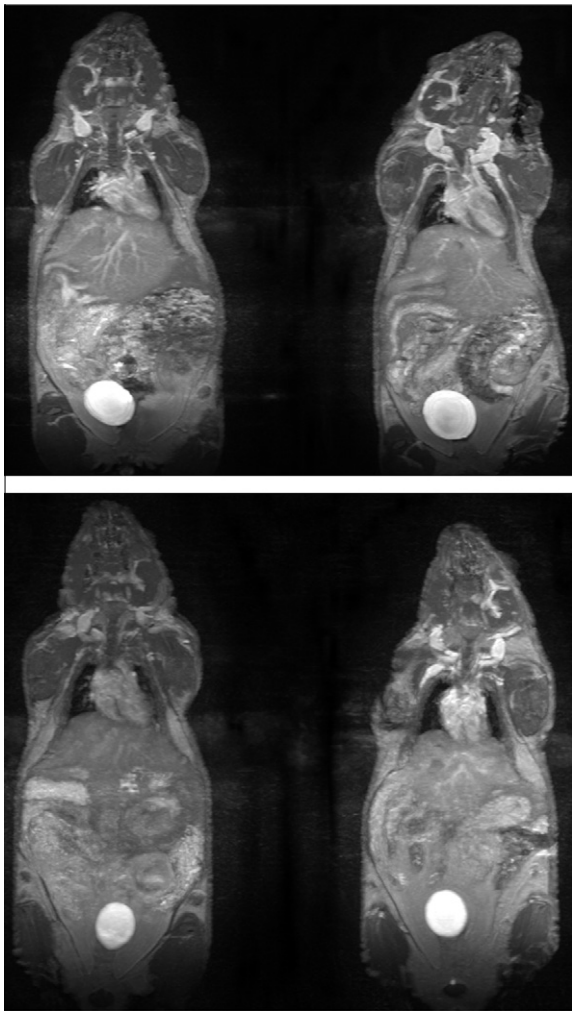

Figure 4. Dynamic MRI of mice injected with 0.015 mmol/kg of G4-(*C*-DOTA-Gd)$_{28}$ (above) and G4-(1B4M-DTPAGd)$_{30}$ (below). All images were acquired at 16–23 min post-injection.

between the positive amine groups and the negative endothelium.[32,33] Also, positively charged macromolecules showed higher glomerular permeation than negatively charged macromolecules with similar molecular weight.[34] We previously reported a higher relaxivity and faster rate of clearance of positively charged macromolecules when compared to negatively charged macromolecules.[25] In general, conjugation of (1B4M-DTPA-Gd)$^{-2}$ (Fig. 6) to a generation 4 dendrimer (G4D) would result in a more hydrophilic conjugate than (*C*-DOTA-[Gd])$^{-1}$ due to the difference in the initial negative charge. Based on the analyses and SE-HPLC data (1B4M-DTPA[Gd])$^{-2}$ occupied 30 out of 64 sites and (*C*-DOTA[Gd])$^{-1}$ occupied only 28, which makes the overall conjugate of G4-(*C*-DOTA-Gd)$_{28}$ more positively charged and thus more hydrophobic as compared to the [G4-(1B4M-DTPA-Gd)$_{30}$]. Note that this analysis neglects association of other ionic species such as Na^+ or Cl^-. Hydrophobic interaction with solvent molecules is known to slow down the tumbling time (τ_R) which results in increase of the relaxivity.[2,35,36] Therefore, a more hydrophobic G4-(*C*-DOTA-Gd)$_{28}$ conjugate is expected to have a faster clearance. The experimental data in Table 1 supports this hypothesis by having a blood clearance half-life of 16.2 min compared to 29.1 min for G4-(1B4M-DTPA-Gd)$_{30}$. A previous study using Gd(DOTA)$^{-1}$ and Gd(DTPA)$^{-2}$ as contrast agents also showed a faster clearance of the former in rat.[24]

We observed that the dendrimer to chelate ratio was 1:30 for the DTPA derivative, which is lower than the previously reported ratio using the post-metallation method (1:57),[26] and 1:28 for the DOTA derivative suggesting the occupation of the chelate approximately at every other terminal of amino surface groups. We were not able to obtain a higher ratio using this pre-metallation method, which could mainly be due to the presence of the metal and the pre-formation of the respective DTPA or DOTA complexes since this variable is the only change being made, albeit this may be more complex than that simple statement. Issues related to flexibility and access to the conjugation sites at the surface of the PAMAM, relative hydrophobicity between ligands versus complexes, and charge for example may all play a part in this observed result. Thus, inclusion of the metal, that is, pre-forming the complex might contribute to or in fact trigger a sterically induced stoichiometry (SIS) condition as pointed out by Tomalia.[37] This lower dendrimer to chelates ratio for the DOTA derivative might generate a more favorable inter-metal distance that retains metal ions to be completely functional and potent with little or no opportunity for any donors to bind to the ninth coordination site of the Gd(III) thereby blocking interaction with H_2O. Previous studies showed that when Gd(III) centers are at close proximity with a short Gd–Gd distance, a significant increase in the electron spin relaxation rates was observed due to the dipole–dipole interactions between Gd spins. Increase in electronic relaxation rate decreases the interaction of the electron spins with the nuclear spin of protons and thus become a limiting factor that leads to lower relaxivity.[38–40] In addition, possession of a short and rigid isothiocyanatobenzyl linker is a positive feature of the conjugate and also a factor that contributes to the high relaxivity among many others.[41] This short and rigid linker limits the rotation of the small Gd(III) chelates, which is characterized as internal rotation. As reported previously, fast internal rotation of high molecular weight

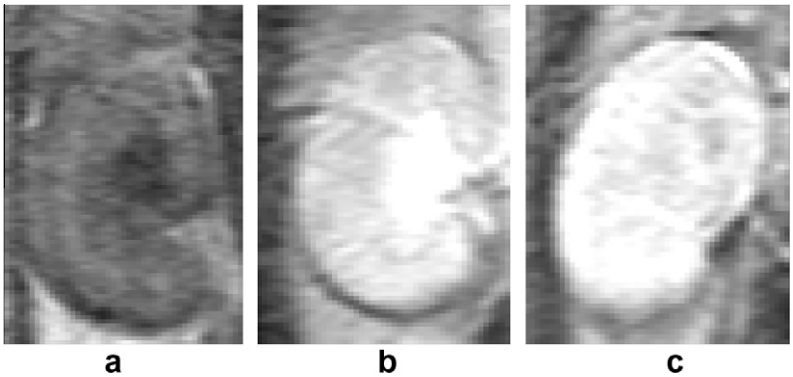

Figure 5. MR images of the left kidney obtained prior to injection of agents (a) and 20 min after injection of G4-(1B4M-DTPA-Gd)$_{30}$ (b) and G4-(*C*-DOTA-Gd)$_{28}$ (c).

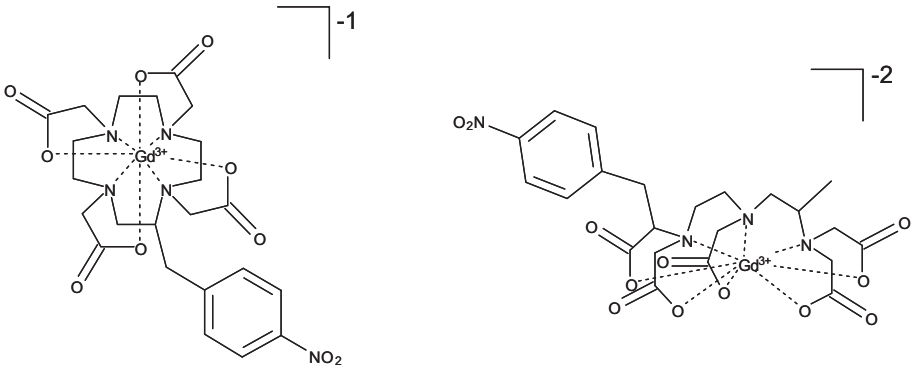

Figure 6. Structures of (*C*-DOTA-Gd)$^{-1}$ (left) versus (1B4M-DTPA-Gd)$^{-2}$ (right).

Table 1
Summary of results for G4-(*C*-DOTA-Gd)$_{28}$ (dota) and G4-(1B4M-DTPA-Gd)$_{30}$ (dtpa)

Agent	G4:chelate	r_1[a] (mM^{-1} s^{-1})	r_2[a] (mM^{-1} s^{-1})	Half life[b] (min)	Rate of clearance[c] (min^{-1})
Dota	1:28	29.5 ± 1.5	61.6 ± 1.7	16.2 ± 1.2	0.063 ± 0.0046
dtpa[d]	1:30	26.9 ± 1.2	56.1 ± 1.4	29.1 ± 0.63	0.034 ± 0.00017

Reported numbers are the average values and errors are reported as standard deviations.
[a] Molar relaxivity values obtained from phantom measurements.
[b] Blood clearance half-life as measured from R_1 map of the jugular vein in dynamic MR angiographic images.
[c] Blood clearance rates.
[d] From Ref. 25.

agents prohibits achievement of high relaxivity even though the rotation of the entire molecule is reasonably slow.[41,42]

The blood clearance plot in Figure 3 illustrates differences in circulation properties between the two agents tested. As expected the rate of clearance of G4-(*C*-DOTA-Gd)$_{28}$ is faster than that of G4-(1B4M-DTPA-Gd)$_{30}$. This enhanced clearance rate eliminates concerns in the aspects of the deposition of the metal chelate in vivo due to a prolonged circulation and residence of the agent, and dissociation of the toxic metal ion from the ligand cavity due to the competition from other anionic ligands in vivo for the metal binding. It also eliminates a concern of in vivo toxicity of cationic PAMAM dendrimers as pointed out by other researchers.[43] In addition, the dose employed for in vivo imaging (0.015 mmol/kg) is much lower than that is required for the clinically approved agents such as Magnevist™ (0.1–0.3 mmol/kg) as well as half of what the majority of our prior studies used with dendrimer agents.[26] This decreased injected dose also reduced the risk of exposure to high amount of toxic metal and also the dendrimer. The data also indicate that there were higher tissue uptakes for G4-(*C*-DOTA-Gd)$_{28}$ that can be useful as a targeting agent. To the best of our knowledge this is the first time MRI properties of two macromolecular agents have been compared.

Gd(DOTA) has been used as a contrast agent to study central nervous system such as intracranial lesions.[44] The result showed that the agent was not only well tolerated but efficient to enhance the contrast of the extracellular space and identify blood brain barrier (BBB) defects. A characteristic that is similar to Gd(DTPA), such as mild contrast uptake in patient with recent cerebellar infarct,[45,46] was also observed. This finding not only reinforces the conclusion that Gd(DOTA) agent is as viable as Gd(DTPA) in MR imaging but also encourages us to consider our stable dendrimer-based Gd-*C*-DOTA conjugate as a potential candidate for brain imaging.

The kidney images for the two agents show differences in diffusion and blood circulation (Fig. 5). G4-(1B4M-DTPA-Gd)$_{30}$ mostly localized around the pelvic area while G4-(*C*-DOTA-Gd)$_{28}$ seems to diffuse throughout. This could be of importance for studies of kidney diseases and kidney damage caused by drugs. A detailed study of drug effect to the kidney using G4-(*C*-DOTA-Gd)$_{28}$ is underway.

5. Conclusion

In conclusion, this study confirms that macromolecular MRI contrast agents composed of multiple Gd(III) chelates assembled on a dendrimer platform are much more efficient and effective in modulating and relaxing water protons as compare to a single chelate unit analogue. Our study also demonstrates that appending the pre-formed DOTA metal complex to the dendrimer is far more convenient and significantly more advantageous in areas including species distribution, ease of characterization, stability, solubility. This pre-metallation method also produces a more hydrophobic agent that results in high relaxivity, faster blood clearance rate in vivo, while also requiring administration of a decreased dose without sacrificing imaging quality. From the data obtained in these studies, we conclude that G4-(*C*-DOTA-Gd)$_{28}$ is a superior agent based on its comparable relaxivity and shorter blood clearance lifetime thereby also advocating elimination of bifunctional DTPA agents for use in the creation of macromolecular MRI contrast agents. By these results, the dendrimer-based agent(s) created employing bifunctional DOTA are far more superior for in vivo applications and will be our major focus in future studies.

Acknowledgments

This research was supported by the Intramural Research Program of the National Institute of Health, National Cancer Institute, Center for Cancer Research and the United States Department of Health and Human Services.

References and notes

1. Caravan, P. *Chem. Soc. Rev.* **2006**, *35*, 512.
2. Wang, S. J.; Brechbiel, M.; Wiener, E. C. *Invest. Radiol.* **2003**, *38*, 662.
3. Kobayashi, H.; Brechbiel, M. W. *Mol. Imaging* **2003**, *2*, 1.

4. Sato, N.; Kobayashi, H.; Hiraga, A.; Saga, T.; Togashi, K.; Konishi, J.; Brechbiel, M. W. *Magn. Reson. Med.* **2001**, *46*, 1169.
5. Tomalia, D. A.; Reyna, L. A.; Svenson, S. *Biochem. Soc. Trans.* **2007**, *35*, 61.
6. Koyama, Y.; Talanov, V. S.; Bernardo, M.; Hama, Y.; Regino, C. A. S.; Brechbiel, M. W.; Choyke, P. L.; Kobayashi, H. *J. Magn. Reson. Imaging* **2007**, *25*, 866.
7. Gillies, E. R.; Fréchet, J. M. J. *Drug Discovery Today* **2005**, *10*, 35.
8. Kukowska-Latallo, J. F.; Candido, K. A.; Cao, Z.; Nigavekar, S. S.; Majoros, I. J.; Thomas, T. P.; Balogh, L. P.; Khan, M. K.; Baker, J. R., Jr. *Cancer Res.* **2005**, *65*, 5317.
9. Gurdag, S.; Khandare, J.; Stapels, S.; Matherly, L. H.; Kannan, R. M. *Bioconjugate Chem.* **2006**, *17*, 275.
10. Lee, C. C.; Gillies, E. R.; Fox, M. E.; Guillaudeu, S. J.; Fréchet, J. M.; Dy, E. E.; Szoka, F. C. *Proc. Natl. Acad. Sci. U.S.A.* **2006**, *103*, 16649.
11. Lee, C. C.; MacKay, J. A.; Fréchet, J. M. J.; Szoka, F. C. *Nat. Biotechnol.* **2005**, *23*, 1517.
12. Chauhan, A. S.; Diwan, P. V.; Jain, N. K.; Tomalia, D. A. *Biomacromolecules* **2009**, *10*, 1195.
13. Supattapone, S.; Nguyen, H.-O. B.; Cohen, F. E.; Prusiner, S. B.; Scott, M. R. *Prog. Nucl. Magn. Reson. Spectrosc.* **1999**, *96*, 14529.
14. Sieber, M. A.; Lengsfeld, P.; Walter, J.; Schirmer, H.; Frenzel, T.; Siegmund, F.; Weinmann, H.-J.; Pietsch, H. *J. Magn. Reson. Imaging* **2008**, *27*, 855.
15. Thakral, C.; Alhariri, J.; Abraham, J. L. *Contrast Media Mol. Imaging* **2007**, *2*, 199.
16. Stratta, P.; Canavese, C.; Aime, S. *Curr. Med. Chem.* **2008**, *15*, 1229.
17. Abrahama, J. L.; Chandrab, S.; Thakrala, C.; Abraham, J. M. *Appl. Surf. Sci.* **2008**, *255*, 1181.
18. Bousquet, J. C.; Saini, S.; Stark, D. D.; Hahn, P. F.; Nigam, M.; Wittenberg, J.; Ferrucci, J. T., Jr. *Radiology* **1988**, *166*, 693.
19. Allard, M.; Doucet, D.; Kien, P.; Bonnemain, B.; Caille, J. M. *Invest. Radiol.* **1988**, *23*, S271.
20. Deray, G.; Bellin, M. F.; Baumelou, B.; Rey, J.-P.; Boulechfar, H.; Grellet, J.; Jacobs, C. *Am. J. Nephrol.* **1990**, *10*, 522.
21. Magerstädt, M.; Gansow, O. A.; Brechbiel, M. W.; Colcher, D.; Baltzer, B.; Knop, R. H.; Girton, M. E.; Naegele, M. *Magn. Reson. Med.* **1986**, *3*, 808.
22. Wang, X.; Jin, T.; Comblin, V.; Lopez-Mut, A.; Merciny, E.; Desreux, J. F. *Inorg. Chem.* **1992**, *31*, 1095.
23. Benazeth, S.; Purans, J.; Chalbot, M.-C.; Nguyen-van-Duong, M. K.; Nicolas, L.; Keller, F.; Gaudemer, A. *Inorg. Chem.* **1998**, *37*, 3667.
24. Runge, V.; Jacobson, S.; Wood, M.; Kaufman, D.; Adelman, L. *Radiology* **1988**, *166*, 835.
25. Nwe, K.; Xu, H.; Regino, C. A. S.; Bernardo, M.; Ileva, L.; Riffle, L.; Wong, K. J.; Brechbiel, M. W. *Bioconjugate Chem.* **2009**, *20*, 1412.
26. Xu, H.; Regino, C. A. S.; Bernardo, M.; Koyama, Y.; Kobayashi, H.; Choyke, P. L.; Brechbiel, M. W. *J. Med. Chem.* **2007**, *50*, 3185.
27. McMurry, T. J.; Brechbiel, M.; Kumar, K.; Gansow, O. A. *Bioconjugate Chem.* **1992**, *3*, 108.
28. Kumar, K.; Tweedle, M. F. *Inorg. Chem.* **1993**, *32*, 4193.
29. Kasprzyk, S. P.; Wilkins, R. G. *Inorg. Chem.* **1982**, *21*, 3349.
30. Lauffer, R. B. *Chem. Rev.* **1987**, *87*, 901.
31. Knop, R. H.; Frank, J.; Dwyer, A.; Girton, M.; Naegele, M.; Schrader, M.; Cobb, J.; Gansow, O.; Maegerstadt, M.; Brechbiel, M.; Baltzer, L.; Doppman, J. *J. Comput. Assist. Tomogr.* **1987**, *11*, 35.
32. Camici, M. *Biomed. Pharmacother.* **2005**, *59*, 30.
33. Adamson, R. H.; Clouch, G. *J. Physiol.* **1992**, *445*, 473.
34. Takakura, Y.; Hashida, M. *Pharmacol. Res.* **1996**, *13*, 820.
35. Kellar, K. E.; Henrichs, P. M.; Hollister, R.; Koenig, S. H.; Eck, J.; Wei, D. *Magn. Reson. Med.* **1997**, *38*, 712.
36. Zech, S. G.; Eldredge, H. B.; Lowe, M. P.; Caravan, P. *Inorg. Chem.* **2007**, *46*, 3576.
37. Tomalia, D. A. *Soft Matter* **2010**, *6*, 456.
38. Nicolle, G. M.; Tóth, E.; Schmitt-Willich, H.; Bernd, R.; Merbach, A. E. *Chem. Eur. J.* **2002**, *8*, 1040.
39. Powell, D. H.; Dhubhghaill, O. M. N.; Pubanz, D.; Helm, L.; Lebedev, Y. S.; Schlaepfer, W.; Merbach, A. E. *J. Am. Chem. Soc.* **1996**, *118*, 9333.
40. Toth, E.; Helm, L.; Merbach, A. E.; Hedinger, R.; Hegetschweiler, K.; Janossy, A. *Inorg. Chem.* **1998**, *37*, 4104.
41. Tóth, E.; Pubanz, D.; Vauthey, S.; Helm, L.; Merbach, A. E. *Chem. Eur. J.* **1996**, *2*, 1607.
42. Koenig, S. H.; Brown, R. D. *Prog. Nucl. Magn. Reson. Spectrosc.* **1990**, *22*, 487.
43. Neerman, M. F.; Zhang, W.; Parrish, A. R.; Simanek, E. E. *Int. J. Pharm.* **2004**, *281*, 129.
44. Parizel, P. M.; Degryse, H. R.; Gheuens, J.; Martin, J.-J.; Vyve, M. V.; De La Porte, C.; Selosse, P.; Van de Heyning, P.; De Schepper, A. M. *J. Comput. Assist. Tomogr.* **1989**, *13*, 378.
45. Virapongse, C.; Mancuso, A.; Quisling, R. *Radiology* **1986**, *161*, 785.
46. Imakita, S.; Nishimura, T.; Naito, H.; Yamada, N.; Yamamoto, K.; Takamiya, M.; Yamada, Y.; Sakashita, Y.; Minamikawa, J.; Kikuchi, H.; Terada, T. *Neuroradiology* **1987**, *29*, 422.